Quantitative Analysis of the Role of Receptor Recycling in T Cell Polarization

Sergey N. Arkhipov and Ivan V. Maly
Department of Computational Biology, University of Pittsburgh School of Medicine, Pittsburg, PA 15260

ABSTRACT Activation of T cells of the immune system involves recognition of the antigen by the T cell receptor and subsequent internalization and recycling of this receptor. We present a numerical model for this process that accounts for the polarity of the intracellular traffic determined by the polarization of the microtubule-organizing center to the immunological synapse. Unexpectedly, the model explains the observed accumulation of receptors at the immunological synapse mainly as dynamic maintenance of the receptor density there, while the surface receptors everywhere else are depleted, even though the internalization occurs primarily at the synapse. In the case of an unsuccessful polarization of the microtubule-organizing center, which alters the polarity of the receptor trafficking, the model explains the absence of receptor accumulation as a dynamic downregulation at the synapse. The experiment shows that in this case the interaction of the T cell with its target is aborted. Disruption of recycling leads in the experiment to accumulation of the incompletely polarized cells. We propose that receptor recycling is a mechanism whereby the cell can sense its internal structure and detect polarity errors, analogous to checkpoint signaling mechanisms that ensure fidelity of cell division.

INTRODUCTION

T cells (TCs) of the immune system perform their functions by interacting directly and individually with antigen-presenting cells (APCs). The interaction leads to activation of the T cells, and depending on the types of cells and molecules involved, may also result in killing (lysis) of the APC, or in its stimulation for antibody production as part of the immune response (1). The molecular recognition of antigen displayed on the surface of the APC is achieved by the T cell receptor (TCR) on the plasma membrane (PM) of the TC. This receptor is constitutively shuttled between the PM and the endocytic recycling compartment (RC) inside the TC (2). Recent experiments showed that recycling the internalized TCR back to the PM is important to achieve the accumulation of this receptor at the TC:APC interface, which can modulate the signal strength (3).

For the TCR recycling, the polarity of the TC cytoskeleton is of importance. The receptor accumulation on the PM in the area of the TC:APC interface (called immunological synapse) is related to the structural polarity of the receptor recycling. Normally, the RC is positioned near the synapse. The RC localization follows the localization of the microtubule-organizing center (MTOC), which is the center of convergence of the microtubule fibers of the TC cytoskeleton (3). The membranous components that belong to the RC are transported along the microtubules to the MTOC (4). Vesicular traffic toward the MTOC is powered by cytoplasmic dynein, whereas the traffic away from the MTOC is powered by another molecular motor, kinesin (5). Vesicles with recycled TCR are transported along the microtubules from the RC to the PM in the area of the immunological synapse, which is proximal to the MTOC and RC (3).

Quantitative studies of the TCR dynamics yielded rate constants for constitutive internalization and for recycling to the PM (6). A kinetic model was formulated that correctly predicted on the basis of these constants the partitioning of the receptor between the PM and RC. This partitioning is determined primarily by the quasi-equilibrium between the internalization and recycling, because the rates of synthesis of the receptors de novo, and of their biochemical degradation, are much lower (2). It has also been found that stimulation of the receptors by the ligand induces internalization with a much higher rate constant than the constitutive one (2,6). The receptor residence time on the PM is 83 min, dropping to 7.8 after stimulation. In the RC, the residence time stays constant at 18 min. The receptor half-life due to degradation, in contrast, is 10.5 h, and although it decreases to 3.5 h after stimulation, the kinetic modeling remains accurate without taking the degradation and de novo synthesis into account (2,6).

In the realistic context of the TC:APC interaction, the receptor ligation only occurs on a part of the PM at the immunological synapse. The previous model considering the PM as one compartment is not strictly applicable to this situation. Analysis of receptor dynamics in this case must also take into account where, relative to the synapse, the recycling is directed by the polar microtubule system. A model that accounts for the polarity of both receptor binding and recycling is presented here that generalizes the previous modeling.

Modeling that accounts for the directionality of the recycling is simplified by the possibility to consider the intracellular transport of the vesicles carrying the receptors between the PM and RC compartments as instantaneous. Like omitting the synthesis and degradation, this is also possible because of

Submitted February 13, 2006, and accepted for publication August 25, 2006.
Address reprint requests to Ivan V. Maly, Tel.: 412-648-7771; E-mail: maly@ccbb.pitt.edu.

0006-3495/06/12/4306/11 $2.00
doi: 10.1529/biophysj.106.083204

the separation of timescales: the velocities of the vesicles moving along the microtubules range between 0.5 and 5 μm/s (7), suggesting travel times <1 min across a TC 15-μm in diameter. As described above, the residence time of the receptors in either PM or RC is, in contrast, 7.8–18 min. One can observe that the travel times are much shorter that the residence times. Therefore, no allowance has to be made in the model for the travel time, whether the receptors are transported to the RC from the neighboring or distant PM regions.

To focus our modeling on the cell-scale redistribution of receptors, we felt compelled to omit the intricate local dynamics of TCR for which a detailed kinetic formalism had already been developed. In particular, concerning ourselves with the overall TCR distribution on the cell scale, we omit the mechanism of segregation of TCR from integrins within the synapse area (8), which has previously been successfully modeled as arising from the bond length differential and membrane bending (9,10). In the interpretation of the results we equate the number of the receptors in the synapse region with the efficiency of the TC:APC interaction, even though not all TCR complexes in the synapse can be stimulated (11–15), and there are many more receptor types that are engaged in the TC:APC interaction (16). Treating the synapse as the uniform domain, we will also assume that all receptors from the synapse area are internalized at the same high rate. In reality there should be a mix of stimulated and unstimulated receptors in the synapse, and only the stimulated ones may be internalized at the high induced rate, while the unstimulated ones may be internalized at the low constitutive rate. By assuming the same high rate for all receptors in the synapse, we follow (for reasons of model simplicity) the comodulation hypothesis as reviewed in Geisler (2). The methodological reason to consider the simplified receptor dynamics was to have an approximately equal level of the kinetic and the spatial detail, given that the structure and kinematics of the TC are understood quantitatively much less than the surface TCR kinetics.

Besides the polarity of the microtubule cytoskeleton that determines the polarity of the recycling, there appear to be two more processes with the potential to significantly impact the cell-scale TCR redistribution after conjugation with an APC that we therefore incorporate in our model: cell surface convection and diffusion. Upon conjugation of the TC with an APC, TCRs in the PM are entrained by a submembrane flow of the actomyosin cortex (17). The flow resulting from the inhomogeneous cortex contraction is directed to the synapse, and even through this flow is transient, lasting only several minutes (18), it may have a significant contribution to the overall TCR redistribution. How the cortex-driven surface TCR flow and the surface diffusion of TCR into the synapse (19) modulate the overall TCR redistribution in addition to the intracellular recycling is a subject of our analysis.

The relatively simple cell-scale model allowed us also to pose an inverse problem: what are the consequences of the modulation of the receptor dynamics by the cytoskeleton polarity for the cytoskeleton polarity itself? Supported by the new experimental data, the kinetic model with the added degree of spatial realism points to some novel mechanisms through which receptor recycling can contribute not only to the polarity of signaling, but indirectly also to the structural polarization of the TC.

MATERIALS AND METHODS

Theoretical models

The model considers the kinetics of redistribution of TCR between four compartments in a TC. One is the intracellular RC. The other compartments are regions of the PM. On the approximately spherical model cell surface, the kinetic model distinguishes between two polar regions and one equatorial region. The subdivision of the PM into the three kinetic compartments is the novel feature of our model that allows us to take into account where the receptors are engaged and where they are recycled in the different experimental situations described below as Models A–G. These specific models predict the dynamics of the same set of variables that are the amounts of receptors in the compartments, as fractions of the total amount of the receptors in a cell. The fraction of receptors in the RC is denoted r, and in the three PM compartments, as p_1, p_2, and p_3. Which compartments are connected by receptor fluxes, and what the corresponding rate constants are, depends on the experimental situation described by the specific model.

Model A (Fig. 1 *a*) is designed to predict the steady-state distribution of receptors in a resting TC, before it encounters the APC. The only internalization mechanism in this case is the slow constitutive internalization. The internalization is modeled as a flux from each of the PM compartments into the RC with the relatively low rate constant $k_c = 0.012$ min^{-1} (2,6). We assume that, as in the TC:APC conjugate, recycling in the resting TC is directed to the area of the PM that is proximal to the asymmetrically located RC. The PM compartment to which the recycling is directed in the resting cell is the polar compartment number 1 (see the diagram in Fig. 1 *a*). The recycling rate constant has been measured as $k_r = 0.055$ min^{-1} (2,6). The surface receptors are redistributed between the PM compartments by diffusion. Given the surface diffusion coefficient (0.12 μm^2/s (19)), the radius of the approximate sphere, which is the PM ($\approx$7.5 μm in Jurkat TCs used in the experiments), and the number of the regions (3), the rate constant of receptor exchange between the neighboring PM compartments can be calculated as $k_d = (0.12\ \mu\text{m}^2/\text{s})/(\pi \times 7.5\ \mu\text{m}/3)^2 \approx 0.117$ min^{-1}. Overall, Model A (resting cell) can be represented by the diagram in Fig. 1 *a* and described by the following equations.

Model A:

$$\begin{aligned} p_1' &= k_d(p_2 - p_1) - k_c p_1 + k_r r, \\ p_2' &= k_d(p_1 - 2p_2 + p_3) - k_c p_2, \\ p_3' &= k_d(p_2 - p_3) - k_c p_3, \\ r' &= k_c(p_1 + p_2 + p_3) - k_r r. \end{aligned}$$

Model B (Fig. 1 *b*) represents a TC in a normal conjugate with an APC. When such a conjugate is formed, the receptors are engaged in the PM area that was opposite the MTOC in the resting cell, which is followed by the MTOC translocation across the TC to the area where the receptors are engaged and the TC:APC synapse is formed (20,21). The RC follows the MTOC (3). To represent this situation, we make four changes in Model A to construct Model B (compare the *diagrams* in Fig. 1, *a* and *b*). Firstly, we identify the PM compartment number 3 with the TC side of the immunological synapse, and change the rate constant of internalization from this compartment to that of the induced internalization, $k_i = 0.128$ min^{-1} (6). Secondly, we direct the recycling from the RC to the PM compartment number 3 to represent the RC reorientation to the synapse. Thirdly, we introduce another term to represent the flow of TCR in the PM with the underlying actomyosin cortex, which is triggered by attachment to the APC. The

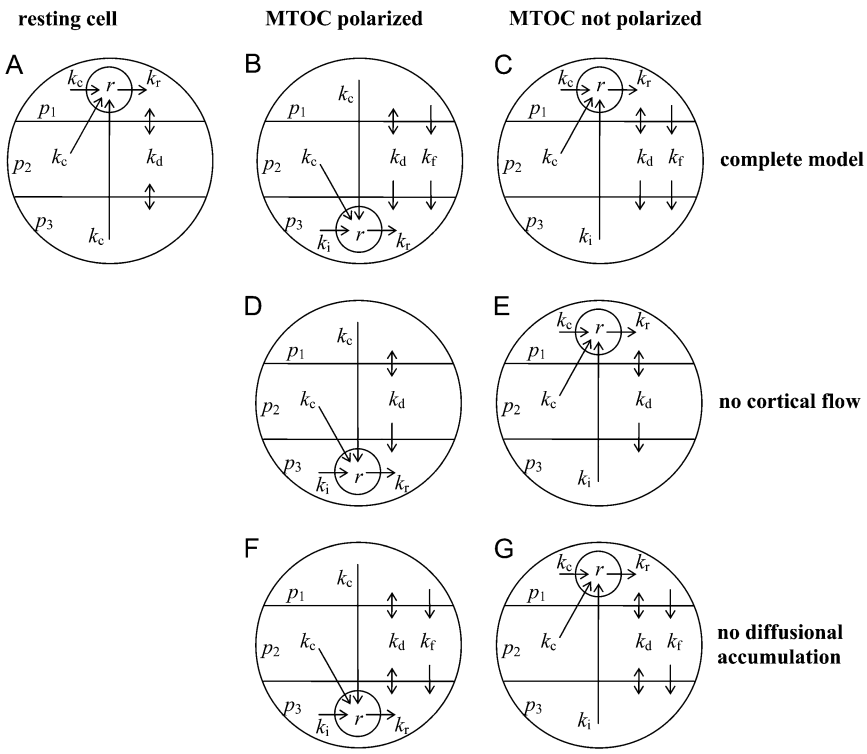

FIGURE 1 Diagrammatic representation of the kinetic models for TCR redistribution in a TC. Four compartments that contain TCR are shown: the intracellular RC (r) and three zones in the PM. The model distinguishes between two opposite polar PM zones p_1 and p_3, and the equatorial PM zone p_2. Arrows show fluxes of TCR between the compartments, each with its associated rate constant k. See Materials and Methods for the detailed explanation and kinetic equations. (*A*) Model A, corresponding to an unstimulated cell. (*B*) Model B, corresponding to a cell that successfully reoriented its MTOC and the associated RC to the PM zone p_3, which is the zone of the immunological synapse. (*C*) Model C, corresponding to a cell that failed to reorient its RC to the immunological synapse p_3. (*D*) Model D, which is a variant of Model B that omits the cortical flow and is used for comparison to determine the contribution of this process to the TCR dynamics. (*E*) Model E, which is a variant of Model C that omits the cortical flow and is used to determine the contribution of this process in the case of the failed MTOC polarization. (*F*) Model F, which is a variant of Model B that omits the diffusional accumulation of TCR in the synapse compartment and is used to determine the contribution of this process into the TCR dynamics. (*G*) Model G, which is a variant of Model C that omits the diffusional accumulation of TCR in the synapse compartment and is used to determine the contribution of this process in the case of the failed MTOC polarization.

rate of this flow decays approximately exponentially with the characteristic time of $\tau_f \approx 2$ min, as seen on the experimental rate versus time plot (18). The initial rate is 0.15 μm/s (18). Recalculating this value as the rate constant of flow between the neighboring PM compartments as done above for the diffusion rate constant, we obtain the initial flow constant of $k_{f0} = (0.15\ \mu\text{m/s})/(\pi \times 7.5\ \mu\text{m}/3) \approx 1.146\ \text{min}^{-1}$. Overall, the time-dependent cortical flow rate constant is defined as $k_f(t) = k_{f0} \times \exp(-t/\tau_f)$. Finally, we postulate that the receptors can diffuse in, but not out, of the synapse compartment to incorporate the diffusion-based mechanism of the receptor accumulation in the synapse (19), which is considered additional to the recycling-based mechanism (3). Model B is represented by the diagram in Fig. 1 *b* and described by the following equations.

Model B:

$$\begin{aligned} p_1' &= k_d(p_2 - p_1) - k_f(t)p_1 - k_c p_1, \\ p_2' &= k_d(p_1 - 2p_2) + k_f(t)(p_1 - p_2) - k_c p_2, \\ p_3' &= k_d p_2 + k_f(t)p_2 - k_i p_3 + k_r r, \\ r' &= k_c(p_1 + p_2) + k_i p_3 - k_r r. \end{aligned}$$

Model C (Fig. 1 *c*) is for the special case of the several percent of TCs that conjugate with an APC, but fail to reorient the MTOC and RC to the synapse (20). Accordingly, Model C is like Model B, except that recycling is directed to the PM compartment 1, as in Model A (as depicted in Fig. 1, *c* compared to *b*). The following equations describe Model C.

Model C:

$$\begin{aligned} p_1' &= k_d(p_2 - p_1) - k_f(t)p_1 - k_c p_1 + k_r r, \\ p_2' &= k_d(p_1 - 2p_2) + k_f(t)(p_1 - p_2) - k_c p_2, \\ p_3' &= k_d p_2 + k_f(t)p_2 - k_i p_3, \\ r' &= k_c(p_1 + p_2) + k_i p_3 - k_r r. \end{aligned}$$

Model D (Fig. 1 *d*) is a variant of Model B (a conjugated TC with a polarized MTOC). The difference between Model D and Model B is that there is no cortical flow in Model D. This model is used for comparison with the complete Model B to evaluate the effect of the cortical flow on the overall TCR redistribution. Model D is described by the following equations.

Model D:

$$\begin{aligned} p_1' &= k_d(p_2 - p_1) - k_c p_1, \\ p_2' &= k_d(p_1 - 2p_2) - k_c p_2, \\ p_3' &= k_d p_2 - k_i p_3 + k_r r, \\ r' &= k_c(p_1 + p_2) + k_i p_3 - k_r r. \end{aligned}$$

Model E (Fig. 1 *e*) has the same relationship to Model C as D has to B. Specifically, Model E differs from Model C (a conjugated TC with a nonpolarized MTOC) in that there is no cortical flow in Model E. Accordingly, Model E is used for comparison with the complete model C to evaluate the effect of the cortical flow in the case of the failed MTOC polarization. Model E is described by the following equations.

Model E:

$$\begin{aligned} p_1' &= k_d(p_2 - p_1)_1 - k_c p_1 + k_r r, \\ p_2' &= k_d(p_1 - 2p_2) - k_c p_2, \\ p_3' &= k_d p_2 - k_i p_3, \\ r' &= k_c(p_1 + p_2) + k_i p_3 - k_r r. \end{aligned}$$

Model F (Fig. 1 *f*) is a variant of Model B (a conjugated TC with a polarized MTOC), in which diffusion out of the synapse zone (p_3) into the equatorial PM zone (p_2) is allowed. This excludes the diffusional accumulation of TCR in the synapse. Accordingly, Model F is used for comparison with the complete Model B to evaluate the effect of the diffusional influx on

the overall TCR redistribution to the synapse. Model F is described by the following equations.

Model F:

$$
\begin{aligned}
p_1' &= k_d(p_2 - p_1) - k_f(t)p_1 - k_c p_1,\\
p_2' &= k_d(p_1 - 2p_2 + p_3) + k_f(t)(p_1 - p_2) - k_c p_2,\\
p_3' &= k_d(p_2 - p_3) + k_f(t)p_2 - k_i p_3 + k_r r,\\
r' &= k_c(p_1 + p_2) + k_i p_3 - k_r r.
\end{aligned}
$$

Model G (Fig. 1 *g*) has the same relationship to Model C as F has to B. Specifically, Model G differs from Model C (a conjugated TC with a nonpolarized MTOC) in that diffusion out of the synapse zone (p_3) into the equatorial PM zone (p_2) is allowed. Accordingly, Model G is used for comparison with the complete Model C to evaluate the effect of the diffusional mechanism of accumulation of TCR in the synapse in the case of the failed MTOC polarization. Model G is described by the following equations.

Model G:

$$
\begin{aligned}
p_1' &= k_d(p_2 - p_1) - k_f(t)p_1 - k_c p_1 + k_r r,\\
p_2' &= k_d(p_1 - 2p_2 + p_3) + k_f(t)(p_1 - p_2) - k_c p_2,\\
p_3' &= k_d(p_2 - p_3) + k_f(t)p_2 - k_i p_3,\\
r' &= k_c(p_1 + p_2) + k_i p_3 - k_r r.
\end{aligned}
$$

The models were solved by the Runge-Kutta method in MathCad software (Mathsoft, Cambridge, MA).

Experimental procedures

Cell culture and microscopy

Jurkat cells (a gift of Dr. L. Kane, University of Pittsburgh) were grown and prepared for observation essentially as described earlier (22). Briefly, the suspension of the cells in RPMI1640 growth medium (Invitrogen, Carlsbad, CA) was transferred onto glass coverslips precoated with anti-TCR mouse IgG1κ antibody (clone UCHT1, BD Pharmingen, San Diego, CA), and allowed to settle and to react with this surface at 37°C. The cells were observed on a Nikon TE 200 inverted microscope (Nikon, Melville, NY) equipped with a ORCA II ERG cooled interline camera (Hamamatsu Photonics, Bridgewater, NJ). The microscope objective was driven by a piezo-positioner PIFOC 721 (Physik Instrumente, Karlsruhe, Germany). The camera, the piezo-positioner, and a Uniblitz shutter (Vincent Associates, Rochester, NY) were coordinated by the IPLab software (Scanalytics, Rockville, MD). The same software was used for image processing and analysis.

Measurement of synapse TCR dynamics

Cells attached to the anti-TCR-coated cover glasses were fixed for 30 min at room temperature in 4% paraformaldehyde (Sigma, St. Louis, MO) and stained with Alexa 488-labeled primary monoclonal anti-CD3 (anti-TCR) mouse antibodies (Invitrogen, 1:100). The cells were then permeabilized in 0.5% Triton (Sigma) for 5 min, and immunostained for microtubules, using mouse anti-tubulin antibodies (Sigma) and TRITC goat anti-mouse antibodies (Invitrogen). The cells were embedded in Antifade medium (Invitrogen) and imaged as described in the previous section, using a 60× Nikon Plan Apo objective (numerical aperture 1.4). Images of optical sections were acquired at 0.4-μm intervals. All cells in each random field of view were categorized as polarized or not polarized. A cell was counted as having a polarized MTOC if the center of convergence of the microtubules was observed within the bottom 2 μm of the cell, as described previously (23). From the *z*-stack acquired on the wavelength of the anti-TCR labeled antibody, a 2-μm-thick optical layer was extracted by summation of six adjacent optical sections encompassing the level at which the cells contact the substrate. In this image, areas were selected within the boundaries of the contact (synapse) area of each cell with the glass. Average fluorescence density within each area was measured and used as the estimate of the TCR density in the synapse of that cell. Background fluorescence density was measured by averaging fluorescence densities in areas unoccupied by cells, and subtracted from the synapse estimates. The percent change in the synapse TCR density was estimated by comparing the average densities in cells fixed 40 min after addition of the suspension to the glass with the average densities in cells fixed 5 min after addition of the suspension. To correlate the TCR dynamics with the MTOC polarization, the percent change was calculated separately for the cells with polarized and nonpolarized MTOC. Duplicate experiments were conducted on separate days.

Measurement of conjugation stability

The cells were incubated with 500 nM Oregon Green 488 TubulinTracker (Molecular Probes, Carlsbad, CA) in the culture medium for 25 min at 37°C and under 5% CO_2 before being injected into the observation chamber (LabTek, Brendale, Austria) as described previously (22). The chamber bottom was a glass coverslip precoated with anti-TCR antibodies as described above. The live cells were imaged through a 60× Plan Apochromat phase-contrast objective with numerical aperture 1.4 (Nikon). The temperature (37°C) was maintained using an ASI 400 air stream incubator (Nevtek, Burnsville, VA). Seventy-six images of the optical sections were taken over 7.5 s beginning every 5 min for 25 min, with a formal resolution (voxel size) of 0.22, 0.22, and 0.4 μm in the *X*, *Y*, and *Z* dimensions, *Z* being along the optical axis and orthogonal to the glass forming the bottom of the observation chamber. The images were taken separately on the wavelength corresponding to the fluorescence of the Oregon Green-labeled microtubules, and in phase contrast. The cells were considered as having the polarized MTOC if they displayed a microtubule aster converging at the bottom of the cell in the entire time sequence of the three-dimensional fluorescent images. Conversely, they were considered as having the nonpolarized MTOC if they displayed a microtubule aster converging at the top of the cell in the entire time sequence. The cells were considered as spread on the chamber bottom at the given time-point if they displayed phase-contrast lamellar protrusions around the cell body, as described earlier (24), in the transmitted-light image taken at that time-point.

Measurement of the effect of brefeldin A

Brefeldin A (an antibiotic used to block the intracellular protein traffic (25)) was purchased from Sigma. It was added to the cell suspension in the growth medium to 10 μg/mL, and the suspension was preincubated for 1 h at 37°C and under 5% CO_2. Control cells were treated identically, except that no drug was added. After the preincubation, the suspension was injected into the observation chambers precoated with anti-TCR antibody, as described above. After 40 min of incubation (37°C, 5% CO_2), the cells attached to the chamber bottom were fixed, permeabilized, and immunostained for microtubules as described in the previous section. Images of optical sections were acquired through a Nikon Plan Apo 100× objective (numerical aperture 1.4) at 0.125-μm intervals. All cells in each random field of view were categorized as polarized or not polarized, as described above. Duplicate controlled experiments were conducted on separate days.

RESULTS AND DISCUSSION

Modeling of the unstimulated cell

The steady-state solution to Model A (Fig. 1 *a*) predicts the following distribution of TCR in a resting TC, as fractions of the total receptor number: $r = 0.18$ in the RC, $p_1 = 0.32$ in

the PM region proximal to the RC, $p_3 = 0.24$ on the opposite PM polar region, and the rest ($p_2 \approx 0.27$) in the equatorial region of the PM. The steady-state fraction in the RC in Model A is very close to the ~15% measured and approximated by the previous model (6). The essentially uniform distribution between the PM regions in our model demonstrates that the previous model, which treated the PM as a single compartment, was adequate in the case of the resting, unconjugated TC. At the same time the absence of a pronounced TCR gradient on the PM in our model does not explain the experimental result that TCs are more sensitive to stimulus at the front than at the rear (26). It is likely, however, that the sensitivity differences in the migrating TC arise from its movement toward or away from the APC rather than from any polarized TCR distribution. The steady-state solution to Model A (unstimulated TC) is used here as an initial condition for computing the dynamic redistribution of the TCR in the TC upon its encountering an APC, in the different situations described by Models B–G.

Modeling of the cell with a polarized MTOC

Model B (Fig. 1 *b*) describes a structurally polarized TC, in which the RC is oriented to the PM region where receptor binding occurs—the immunological synapse. The internalization of the receptor from the synapse region (the surface region p_3 in the model) proceeds at the increased rate of the stimulated endocytosis. The time course of the receptor levels in all the compartments is shown in Fig. 2 *b*. It displays gradual accumulation of receptors in the intracellular RC (r), from 0.18 to 0.70 of the total amount. This means that the complementary fraction of receptors in all of the PM regions combined ($p_1 + p_2 + p_3$) drops from the initial 0.82 to 0.30. This dramatic drop of the number of TCRs on the cell surface during the first few minutes after conjugation was observed in experiments (e.g., (27)). Distinguishing between the PM regions, our model predicts that while the receptor level indeed drops precipitously in the PM areas (p_1 and p_2) other than the synapse, it in fact increases sharply in the synapse (p_3) during the first 2.4 min, reaching 0.51, which is more

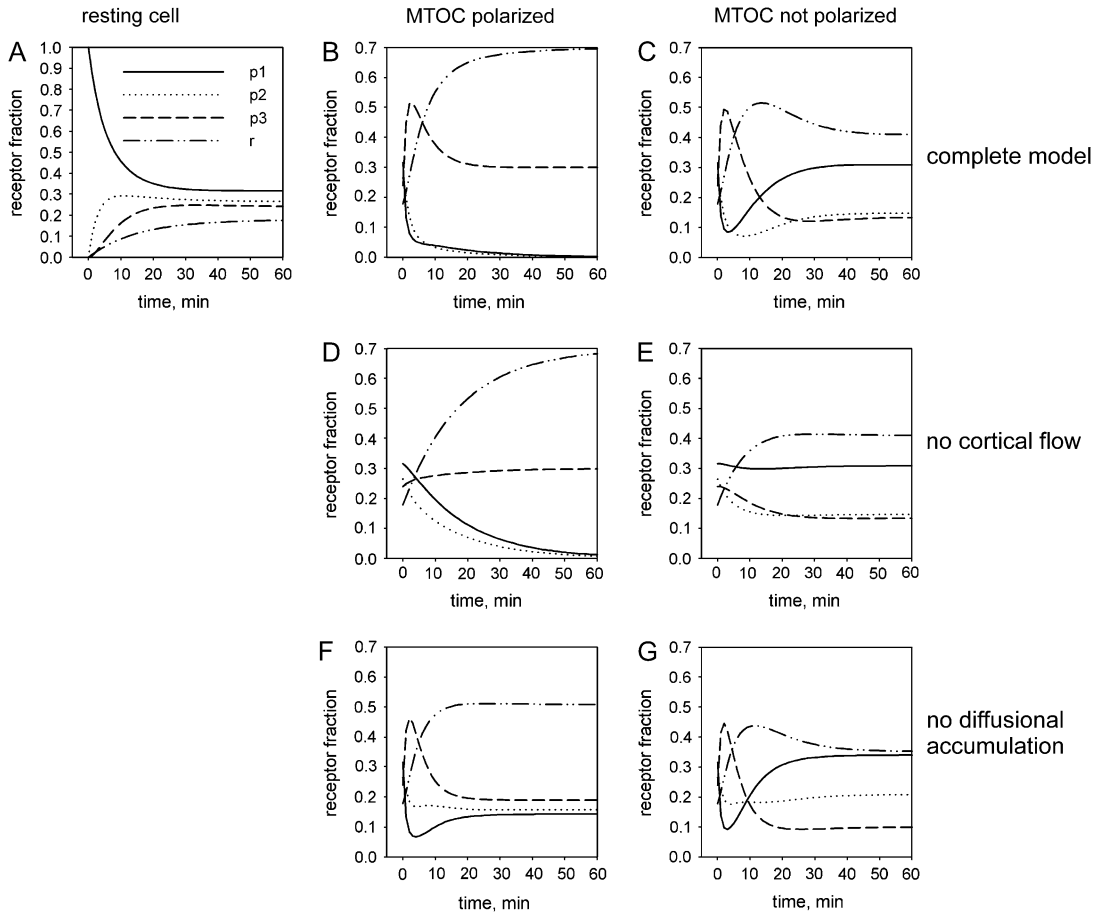

FIGURE 2 Redistribution of TCR between the intracellular pool (r) and the different regions on the PM (p_1, p_2, p_3), of which p_3 corresponds to the immunological synapse, p_1 to the opposite pole of the cell, and p_2 to the equatorial region. The figure parts (*A–G*) correspond to Models A–G, the kinetic diagrams of which are shown in corresponding panels of Fig. 1. Part *A* here contains the curve labels, and also shows the equilibration in an unstimulated cell from an arbitrary initial condition, demonstrating how the steady state is reached which is used as the initial condition in all the models of the stimulated cell (*B–G*). Parts *B–G* show redistribution in a stimulated cell, in the different models and situations as labeled.

than double the initial level in the synapse region (0.24). The TCR level in the synapse then decays quasi-exponentially, approaching within 40 min the new steady-state level of 0.30. This is only 25% higher than the initial TCR level in the synapse, but the rest of the PM by that time contains virtually no TCR, according to the model.

Comparison with the results from Model D (Figs. 1 *d* and 2 *d*), in which there is no cortical flow of the receptors, demonstrates that the initial rise of the TCR level in the synapse in the complete Model B was due to the cortical flow. The longer-term behavior of Models B and D is very similar, so the choice between them should be made based on whether the TCR dynamics immediately after conjugation with the APC (17,18) needs to be reproduced. In contrast, Model F, in which no diffusional accumulation in the synapse is postulated (Fig. 1 *f*), predicts that the new steady-state synapse TCR level in the activated cell is lower (by 21%) than the initial level, and the other PM regions retain so much surface TCR that its polarization to the synapse is not very pronounced in the long term (Fig. 2 *f*). This low degree of surface TCR polarization is most likely incompatible with its detection in the experiment (3). Although allowing diffusion in, but not out, of the synaptic PM region is a crude model for the diffusional mechanism of accumulation of receptors in the synapse PM region (19), our modeling suggests that the diffusional influx plays an important role in the overall TCR polarization in activated TC. On the basis of the comparison of the three models (B, D, F), Model B can be selected as the general model for a TC that has conjugated with an APC and polarized its MTOC to the immunological synapse.

On the basis of the analysis of Model B, it can be concluded that the induced internalization from the synapse region is slightly offset, in the long term, by the recycling which is directed to this region because of the RC polarity, and by the diffusional influx from the rest of the PM. Accumulation of receptors in the synapse relative to the rest of the PM was reported (3,28,29), although the methods used (fluorescent staining) do not give absolute numbers. The model explains the observed relative accumulation mainly by dynamic maintenance, through balanced internalization and reexpression, of the receptor level at the synapse, whereas the rest of the PM loses receptors ultimately to the intracellular pool. This is unexpected and stresses the need for absolute measurements of the receptor levels in the different parts of the TC.

Modeling of the cell with a nonpolarized MTOC

Model C (Fig. 1 *c*) represents an abnormal situation wherein the MTOC and the associated RC fail to reorient to the immunological synapse, which is observed in several percent of cells (20). The polarization failure should render the TC incapable of exocytosis of the vesicles with effector molecules in the direction of the APC, making the TC:APC interaction nonfunctional and possibly damaging to the bystander cells in the tissue because the exocytosis of the effectors would be misdirected (21,30). In Model C, representing the failure to reorient the MTOC and the associated RC, the induced internalization at the higher rate removes receptors from the synapse compartment of the PM (p_3), as in Model B, but the recycling is directed to the opposite pole of the surface (p_1), as in Model A. To be engaged in the cell-cell interaction, the receptors must return to the synapse (p_3) by diffusion through the equatorial region of the PM (compartment p_2). The time course of the receptor redistribution in Model C (Fig. 2 *c*) demonstrates that the balance of internalization and re-expression at the synapse is upset, causing the receptor level in that compartment of the model (p_3) to decrease. Thus, Model C reproduces the experimentally detected impairment of the receptor accumulation at the synapse in cells with impaired orientation of the RC (3). Fig. 3 highlights the contrast between the dynamics of TCR in the synapse, predicted when the RC and MTOC are properly polarized to the synapse (Model B) and when they are not (Model C).

The magnitude of the decrease to the new steady-state level is the same, 45%, whether it follows an initial spike due to the cortical flow in model C (Fig. 2 *c*) or is monotonic in Model E, which omits the cortical flow for comparison (Figs. 1 *e* and 2 *e*). The decrease is slightly more pronounced, 60%, in Model G, which omits the diffusional mechanism of accumulation in the synaptic PM region (Figs. 1 *g* and 2 *g*). The comparison between the three models for the cell that fails to polarize its MTOC (C, E, G) largely parallels the comparison between the models for the cell that completes the MTOC polarization (B, D, F). It similarly demonstrates that the transient cortical flow of TCR is important only for the early phases of TCR redistribution. However, when the MTOC is not polarized, the diffusional influx into the synaptic

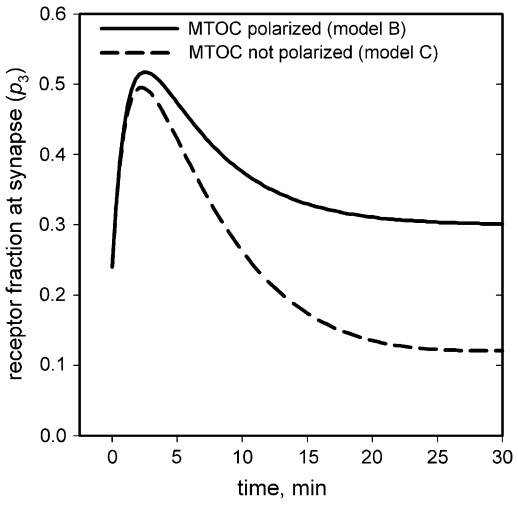

FIGURE 3 The time courses of the receptor fraction in the synapse when the MTOC is polarized (Model B) and not polarized (Model C) are plotted on the same graph for comparison.

PM region has but a marginal effect. On the theoretical grounds, we would be justified in selecting, as the model for the cell that fails to polarize its MTOC, Model C for being the mechanistic counterpart of Model B that was preferred as the model for the normally polarized TC. More precise experimental measurements, however, are necessary to differentiate between the alternative models more reliably.

Measurements of synapse TCR dynamics

In the light of the model predictions, it becomes important that strictly speaking, in the cited experiments (3), the population of cells with experimentally randomized orientation of the RC still exhibited an increase in the receptor density on the synapse, albeit the increase was less expressed compared to the control population, which normally consists mostly of the correctly polarized cells. In Model C, in comparison, the cell has the reverse polarity of the microtubule cytoskeleton and receptor traffic, and the receptor density on the synapse decreases as a result. It is conceivable that the decrease of the receptor accumulation in the randomized population is due to the presence of the cells that are structurally organized and behave as in Model C and therefore exhibit the receptor depletion rather than the reduced accumulation. The model results stress the need for experiments focusing on individual cells.

We measured experimentally the accumulation of TCR at the interface between a Jurkat TC and glass coated with antibodies to TCR. The antibodies stimulate the receptor, and the artificial surface mimics the surface of an APC in this experimental model of the TC:APC interaction (31,32). The Jurkat cells in this experimental system behave similarly to TCs forming conjugates with real APCs, exhibiting, in particular, the polarization of the MTOC to the cell-glass interface that shows some properties of the immunological synapse, and the dramatic expansion of this interface through spreading of the cell on the anti-TCR surface (23,24,33). We were able to determine simultaneously the position of the MTOC and the surface TCR distribution in individual cells (Fig. 4, *a* and *b*). In 40 min after applying the cell suspension to the biomimetic surface, almost all cells (96.3%, $n = 1162$) exhibited the polarized position of the MTOC near the stimulating substrate. The MTOC in the few other cells was not polarized, occupying a position high above the substrate (compare the cells in Fig. 4 *a*). This variation in the cell population is essentially the same as in the previous experiments (20,23). Also as described before (e.g., (3)), the surface TCR distribution exhibited inhomogeneities, which were, to a degree, correlated visually with the position of the MTOC (compare Fig. 4, *a* and *b*). Measurements were necessary to assess the functionally significant correlation of the receptor density at the synapse surface with the orientation of the MTOC in individual cells.

We measured the TCR density on the cell surface facing the stimulatory substrate (the model immunological synapse) separately in cells with polarized and nonpolarized MTOC. By 40 min after plating, the cells with the polarized MTOC elevated their synapse receptor density by 27.1 ± 6.6% ($n = 1641$). The accumulation is in agreement with the previous observations (3). In contrast, the synapse TCR density in the cells whose MTOC failed to polarize dropped 34.1 ± 10.0% ($n = 194$, Fig. 4 *c*). As discussed above, the measurements

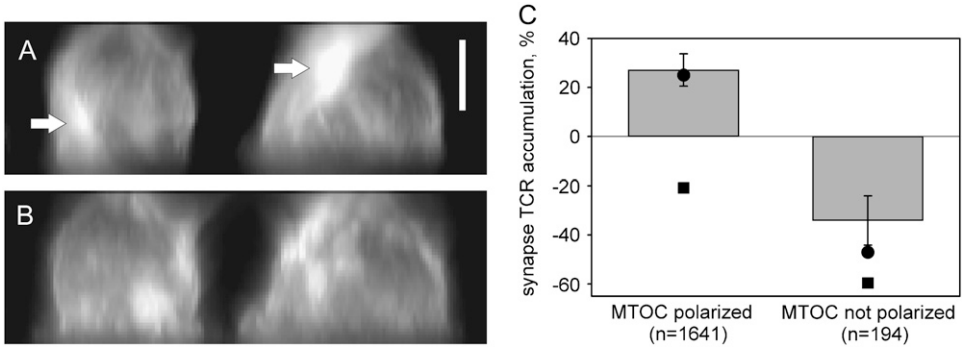

FIGURE 4 Correlation of the TCR dynamics in the synapse with the polarization of the MTOC. (*A*) Side view of a three-dimensional reconstruction of microtubule fluorescence in two TCs attached to the stimulatory substrate below. The fluorescent microtubules converge on the MTOC, making it the brightest area in each cell (*arrows*). The MTOC is polarized to the underlying APC-mimicking substrate (to the synapse) in the cell on the left. In the cell on the right, the MTOC is not polarized to the synapse, and is lying high above the substrate. Scale bar, 5 μm. (*B*) Side view of a three-dimensional reconstruction of surface TCR fluorescence in two TCs attached to the stimulatory substrate below. The cells, their orientation, and the image frame are the same as in part *A* of this figure. (The direct TCR immunofluorescent staining was done before cell permeabilization, therefore only surface TCR is fluorescently labeled in this image. Notice that this is not a conventional, single optical section but a side view of a complete three-dimensional reconstruction that shows the TCR distribution on cell surface in its entirety. Therefore, parts of the cell outline may appear slightly brighter because there is more surface there that is projected along the line of sight. Also, the image area within the cell outline is not dark because there the line of sight crosses the cell surface twice, before and after passing through the unlabeled interior of the cell.) It can be seen that the TCR distribution on the cell surface is not uniform. In the cell on the right, the surface TCR seems to concentrate on the same side of the cell where the MTOC is located, high above the substrate (compare with panel *A* of this figure). In the cell on the left, the surface TCR appears to be concentrated near the bottom of the cell attached to the substrate below. This corresponds to the polarization of the MTOC in this cell (see part *A*) to the substrate, although the peak of the TCR labeling does not exactly coincide with the location of the centrosome in this cell. (*C*) Measurements of the relative change in the TCR contents in the synapse area in 40 min after plating cells on the stimulatory substrate (*bars*). (*Circles*) Prediction of the complete model (Model B for the polarized MTOC and Model C for the nonpolarized MTOC). (*Squares*) Prediction of the model that omits the diffusional accumulation of TCR in the synapse (Model F for the case of the polarized MTOC and Model G for the case of the nonpolarized MTOC).

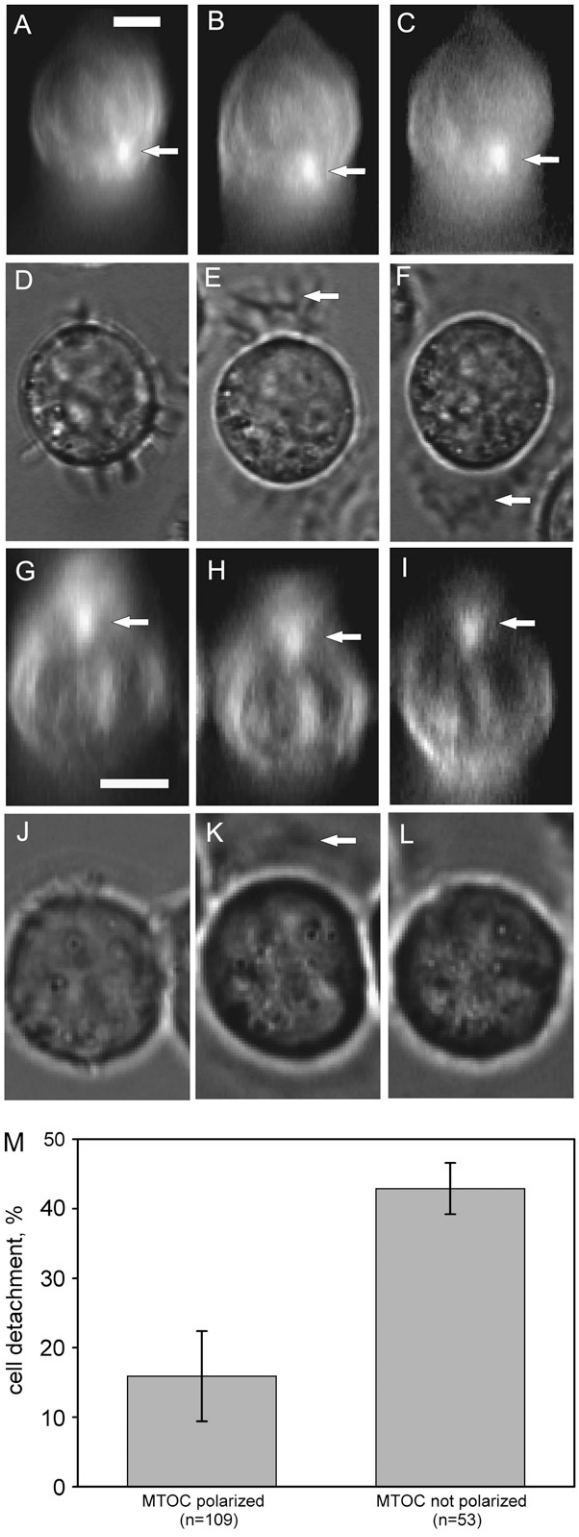

FIGURE 5 Correlation of the stability of TC attachment to the anti-TCR-coated stimulatory substrate with the MTOC polarization. (*A–C*) Sequential (at 2, 10, and 25 min after plating) side views of a three-dimensional reconstruction of microtubule fluorescence in a live TC on the stimulatory substrate below. The fluorescent microtubules converge on the MTOC, making it the brightest area in each cell (*arrows*). The MTOC is polarized to the underlying APC-mimicking substrate (to the synapse). Scale bar, 5 μm. (*D,E*) Phase-contrast top views of the same cell as in panels *A–C* and at the same time-points. The cell body is surrounded by protrusions that form large, flat lamellipodia extended over the substrate in 10 min (panel *E*, one lamellipodium indicated by an *arrow*) that persist through 25 min (panel *F*, one lamellipodium indicated by an *arrow*). (*G–L*) These panels are analogous to panels *A–F*, but show a cell whose MTOC is not polarized to the substrate. Lamellipodia extending over the substrate are seen at the 10-min time-point (panel *K*), but retract by 25 min (panel *L*). (*M*) Measurements of the cell detachment (lamellipodia retraction) from the substrate within 10 min after the cell is first seen sending out the lamellipodia over the substrate.

made on populations of cells whose MTOC position was randomized by colchicine treatment showed only a decrease in accumulation (3). Our measurements on individual untreated cells demonstrate that the relatively rare cells whose MTOC is not polarized due to natural polarization failure display an actual decrease in the synapse TCR density, not a lower degree of increase. This is as predicted by our mathematical model (Fig. 3).

The mathematical model predicts the decrease in the synapse TCR density in the cells that fail to polarize their MTOC irrespective of what is assumed about diffusional accumulation of TCR in the synapse (Fig. 2). If there is no diffusional mechanism of accumulation in the synapse, the synapse TCR density in cells with nonpolarized MTOC is predicted to fall in 40 min by 60% (Model G, Fig. 2 *g*). If the diffusional accumulation in the synapse is assumed, the synaptic TCR level will fall by 47% (Model C, Fig. 2 *c*). The latter prediction is closer to the experimental 34.1 $\pm$ 10.0% (Fig. 4 *c*), which argues once more in favor of the diffusional accumulation hypothesis (19). However, the data differentiate better yet between the models for cells with polarized MTOC. In this case, the synapse TCR density is predicted to decrease by 21% if there is no diffusional accumulation in the synapse (Fig. 2 *f*), but it should increase by 25% if the diffusional accumulation is assumed (Fig. 2 *b*). Only the prediction of the model with the diffusional accumulation (B, not F) is in agreement with the data on the cells with polarized MTOC (Fig. 4 *c*). We conclude that the hypothesis that TCR accumulates in the synapse by diffusion (which implies that at least on balance it diffuses in, but not out of the synapse, (19)) explains the new data better. This substantiates our selection of Model B as the preferred model for the TC with a polarized MTOC, and of Model C as its mechanistic counterpart for the TC with a nonpolarized MTOC. At the same time, we emphasize that in the more general sense, the predicted correlation of the synapse TCR dynamics with MTOC polarization is independent of the controversy over whether TCR accumulates at least in part by diffusion, because even though the model without the diffusional accumulation mechanism predicts some decrease in the synapse TCR density in cells with properly polarized MTOC, the decrease is predicted to be threefold deeper in cells whose MTOC does not polarize (Fig. 2, *f* and *g*).

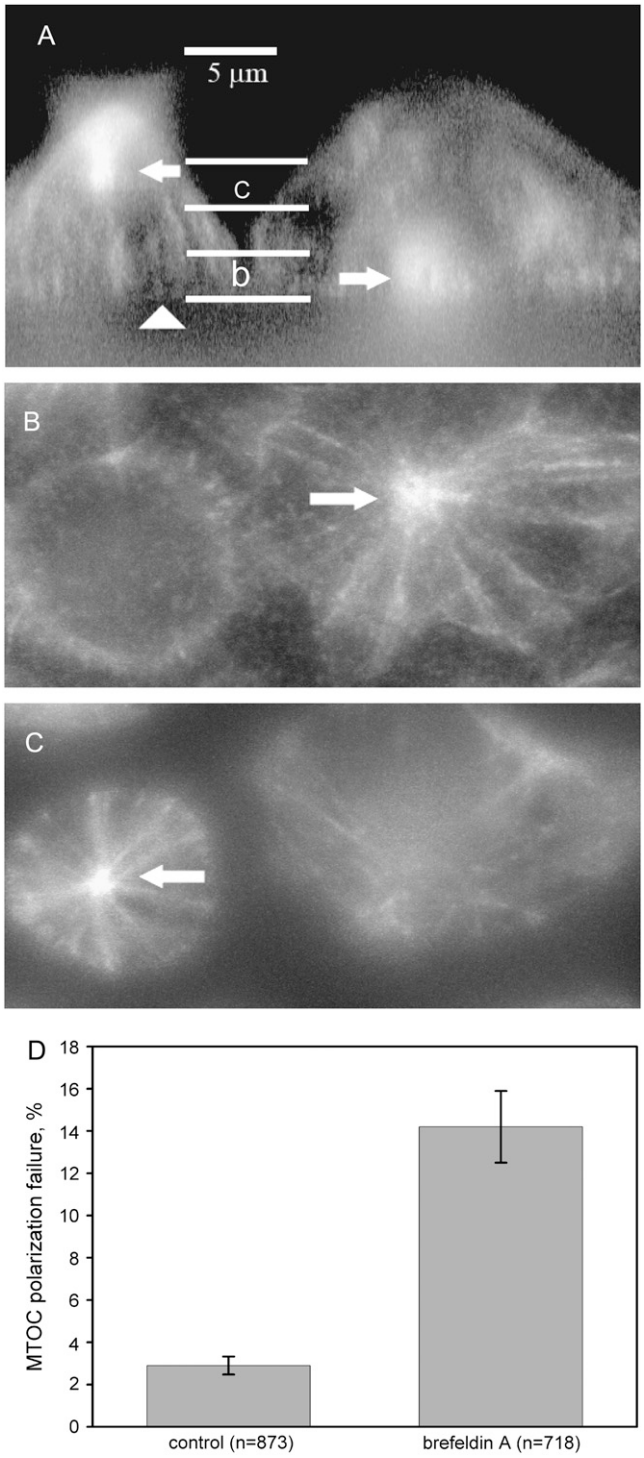

FIGURE 6 Dependence of the failure rate of MTOC polarization on TCR recycling. (*A–C*) Cells pretreated with brefeldin A to disrupt TCR recycling, which caused a high frequency of MTOC polarization failure. (*A*) Side view of a three-dimensional reconstruction of microtubule fluorescence in two TCs attached to the stimulatory substrate below. The fluorescent microtubules converge on the MTOC, making it the brightest area in each cell (*arrows*). The MTOC is polarized to the underlying APC-mimicking substrate (level indicated by the *arrowhead*) in the cell on the right. In the cell on the left, the MTOC is not polarized to the synapse and is lying high above the substrate. Scale bar, 5 μm. The two pairs of horizontal lines indicate the boundaries of the two horizontal layers that are shown in panels *B* and *C*. (*B*) Top view of the stack of optical sections in the lower parts (next to the substrate and synapse) of the same cells as in panel *A*. The MTOC is indicated by the arrow. The vertical boundaries of the layer shown are indicated in panel *A* by letter *b*. (*C*) Top view of the stack of optical sections in the upper (farther from the substrate and synapse) parts of the same cells as in panel *A*. The vertical boundaries of the layer shown are indicated in panel *A* by letter *c*. The MTOC is indicated by the arrow. (*D*) Measurements of the fraction of cells that fail to polarize their MTOC to the synapse with the stimulatory substrate in 40 min after plating.

Measurements of the differential stability of TCR-mediated conjugation

To determine if the depletion of receptors from the synapse can cause disengagement from the target surface in the case of the MTOC polarization error, we followed individual live cells in the same experimental model. Cells that fail to orient the MTOC to the interface with the anti-TCR surface exhibit a higher rate of retraction of the cell surface from the anti-TCR glass after the initial spreading (Fig. 5). Note that 42.9 $\pm$ 0.7% ($n = 53$) of the cells with the misoriented MTOC retracted in 10 min after spreading, compared to only 15.9 $\pm$ 1.2% ($n = 109$) of the correctly polarized cells. This may represent the active abortion by a TC of its response to the stimulus when the cell detects the polarization error.

It was shown previously that experimental disassembly of microtubules makes the Jurkat TCs unable to efficiently accumulate TCR at the immunological synapse they form with APCs (3), as well as reduces the stability of the contact they develop with the anti-TCR coated biomimetic surface (24). At the same time, the microtubule disassembly prevents polarization of the MTOC (21) and of the RC (3) associated with the MTOC. Our results are consistent with these data which were obtained on whole populations of cells subjected to experimental intervention and then to chemical fixation for one-time observation. By revealing the dynamics of the individualized responses live cells exhibit when subjected to identical treatment and tracked over time, our data demonstrate in addition that the contact stability in a responding TC is reduced when the polarization of an intact microtubule cytoskeleton is not accomplished by this particular cell.

Measurement of the effect of recycling on MTOC polarity

The lower stability of the TCR-mediated conjugation with the APC-mimicking surface, which is exhibited by cells with the incorrectly polarized MTOC (Fig. 5) could, in theory, keep their numbers down in the total population of the conjugated cells. This would constitute effectively a TCR recycling-based mechanism of MTOC polarization in TCs: although it does not move the MTOC physically, it eliminates cells that do not polarize their MTOC from the conjugated cell population. To determine if such a recycling-based mechanism plays a role in the overall MTOC polarization,

we compared the normal degree of MTOC polarization in the conjugated cell population with the degree of polarization that is achieved when the TCR recycling is disrupted.

We employed brefeldin A, which was previously shown to disrupt TCR recycling (34) and to impair the accumulation of TCR at the synapse via the directed recycling (3). In our model of recycling as well as in the measurements (Fig. 3 and Fig. 4 *c*), the cells with correctly polarized MTOC accumulate TCR at the synapse, whereas the cells with nonpolarized MTOC do not. Consequently, impairing the synapse TCR accumulation with brefeldin A would eliminate the advantage of the higher synapse TCR density and contact stability that is normally held by the cells with polarized MTOC. If so, the share of cells with nonpolarized MTOC in the total conjugated cell population should then noticeably increase.

In close agreement with the previous measurements (20,23), we find that under the control conditions, the MTOC is not polarized to the synapse in 2.9 $\pm$ 0.4% of the cells conjugated with the TCR-binding surface in 40 min after the beginning of the experiment ($n = 873$). Pretreatment of the cells with brefeldin A increases the fraction of cells with nonpolarized MTOC to 14.2 $\pm$ 1.7% ($n = 718$, Fig. 6), as expected under our hypothesis. We conclude that TCR recycling plays an indirect, but significant role in MTOC polarization through the differential retention of the correctly polarized cells in the population of cells conjugated with the TCR-engaging surface.

CONCLUSIONS

The kinetic modeling indicates that the receptor numbers are slightly increased and then maintained in the PM region of the immunological synapse, if the RC associated with the MTOC is successfully translocated there from the opposite pole of the TC. This is in agreement with the data indicating the role of the directed recycling in ensuring sustained signaling through the TCR (3). The failure of the TC to achieve the MTOC polarity necessary for the directed delivery of the effector molecules to the APC (21,30), which is observed in several percent of intact cells (20), leads, according to the previous data, to a failure to polarize the TCR distribution to the synapse (3). Our kinetic model reproduces this phenomenon as well. The new experimental data presented here demonstrate that, in the case of the failed polarization, the contact of the TC with the TCR-binding surface is abnormally prone to collapsing. This can keep down the number of TC-APC conjugates with the incorrect MTOC polarity. The hypothesis is consistent with the higher MTOC polarization error rate exhibited by cells with experimentally disrupted TCR recycling.

Signaling mechanisms that detect an incorrect assembly of the mitotic spindle abort abnormal cell divisions that would, if allowed to proceed, give genetically defective daughter cells (7). Our theoretical and experimental results indicate that TCR recycling can serve as a mechanism sensitive to the structural polarity of the TC and trigger disengagement of TC-APC pairs that would otherwise be unproductive or damaging to bystander cells because of the misorientation of the MTOC in the TC (30). Unlike the ''checkpoint'' mechanisms in mitosis that postulate, for example, mechanosensitive proteins (35), the mechanism proposed here does not involve any sensor molecule. It is the redistribution of the signaling components on the scale of the entire cell, depending on the cell-scale structure, which is responsible for the decision to sustain or abort the immune cell-cell interaction in this case. In terms of the proposed mathematical model, the structural state of the cell influences signaling through the topology of reactions connecting different signaling domains, rather than through any change in the kinetic constants. Arguably, this makes the ability of the cell to sense its own structure a function of the entire system rather than of any of its molecular components.

Supported by National Institutes of Health grant No. GM078332 to I.V.M.

REFERENCES

1. Alberts, B., K. Roberts, J. Lewis, M. Raff, and D. Bray. 1989. Molecular Biology of the Cell, 2nd Ed. Garland, New York.
2. Geisler, C. 2004. TCR trafficking in resting and stimulated T cells. *Crit. Rev. Immunol.* 24:67–86.
3. Das, V., B. Nal, A. Dujeancourt, M.-I. Thoulouze, T. Galli, P. Roux, A. Dautry-Varsat, and A. Alcover. 2004. Activation-induced polarized recycling targets T cell antigen receptors to the immunological synapse: involvement of SNARE complexes. *Immunity.* 20:577–588.
4. Burkhardt, J. K., C. J. Echeverri, T. Nilsson, and R. B. Vallee. 1997. Overexpression of the dynamitin (p50) subunit of the dynactin complex disrupts dynein-dependent maintenance of membrane organelle distribution. *J. Cell Biol.* 139:469–484.
5. Goodson, H. V., C. Valetti, and T. E. Kreis. 1997. Motors and membrane traffic. *Curr. Opin. Cell Biol.* 9:18–28.
6. Menne, C., T. Sorensen, V. Siersma, M. von Essen, N. Odum, and C. Geisler. 2002. Endo- and exocytic rate constants for spontaneous and protein kinase C-activated T cell receptor cycling. *Eur. J. Immunol.* 32:616–626.
7. Bray, D. 2001.Cell Movements: From Molecules to Motility. Garland, New York.
8. Monks, C. R., B. A. Freiberg, H. Kupfer, N. Sciaky, and A. Kupfer. 1998. Three-dimensional segregation of supramolecular activation clusters in T cells. *Nature.* 395:82–86.
9. Qi, S. Y., J. T. Groves, and A. K. Chakraborty. 2001. Synaptic pattern formation during cellular recognition. *Proc. Natl. Acad. Sci. USA.* 98: 6548–6553.
10. Burroughs, N. J., and C. Wülfing. 2002. Differential segregation in a cell-cell contact interface: the dynamics of the immunological synapse. *Biophys. J.* 83:1784–1796.
11. Coombs, D., A. M. Kalergis, S. G. Nathenson, C. Wofsy, and B. Goldstein. 2002. Activated TCRs remain marked for internalization after dissociation from pMHC. *Nat. Immunol.* 3:926–931.
12. Wofsy, C., D. Coombs, and B. Goldstein. 2001. Calculations show substantial serial engagement of T cell receptors. *Biophys. J.* 80: 606–612.
13. Gakamsky, D. M., I. F. Luescher, A. Pramanik, R. B. Kopito, F. Lemonnier, H. Vogel, R. Rigler, and I. Pecht. 2005. CD8 kinetically

promotes ligand binding to the T-cell antigen receptor. *Biophys. J.* 89:2121–2133.

14. Gonzalez, P. A., L. J. Carreno, D. Coombs, J. E. Mora, E. Palmieri, B. Goldstein, S. G. Nathenson, and A. M. Kalergis. 2005. T cell receptor binding kinetics required for T cell activation depend on the density of cognate ligand on the antigen-presenting cell. *Proc. Natl. Acad. Sci. USA.* 102:4824–4829.
15. Lee, K.-H., A. R. Dinner, C. Tu, G. Campi, S. Raychaudhuri, R. Varma, T. N. Sims, W. R. Burack, H. Wu, J. Wang, O. Kanagawa, M. Markiewicz, P. M. Allen, M. L. Dustin, A. K. Chakraborty, and A. S. Shaw. 2003. The immunological synapse balances T cell receptor signaling and degradation. *Science.* 302:1218–1222.
16. Sancho, D., M. Vicente-Manzanares, M. Mittelbrunn, M. C. Montoya, M. Gordon-Alonso, J. M. Serrador, and F. Sanchez-Madrid. 2002. Regulation of microtubule-organizing center orientation and actomyosin cytoskeleton rearrangement during immune interactions. *Immunol. Rev.* 189:84–97.
17. Wülfing, C., and M. M. Davis. 1998. A receptor/cytoskeletal movement triggered by costimulation during T cell activation. *Science.* 282: 2266–2269.
18. Moss, W. C., D. J. Irvine, M. M. Davis, and M. F. Krummel. 2002. Quantifying signaling-induced reorientation of T cell receptors during immunological synapse formation. *Proc. Natl. Acad. Sci. USA.* 99: 15024–15029.
19. Favier, B., N. J. Burroughs, L. Wedderburn, and S. Valitutti. 2001. TCR dynamics on the surface of living T cells. *Int. Immunol.* 13:1525–1532.
20. Geiger, B., D. Rosen, and G. Berke. 1982. Spatial relationships of microtubule-organizing centers and the contact area of cytotoxic T lymphocytes and target cells. *J. Cell Biol.* 95:137–143.
21. Kupfer, A., and S. J. Singer. 1989. Cell biology of cytotoxic and helper T cell functions: immunofluorescence microscopic studies of single cells and cell couples. *Annu. Rev. Immunol.* 7:309–337.
22. Bunnell, S. C., V. A. Barr, C. L. Fuller, and L. E. Samelson. 2003. High-resolution multicolor imaging of dynamic signaling complexes in T cells stimulated by planar substrates. *Sci. STKE.* 2003:pl8.
23. Kuhne, M. R., J. Lin, D. Yablonski, M. N. Mollenauer, L. I. R. Ehrlich, J. Huppa, M. M. Davis, and A. Weiss. 2003. Linker for activation of T cells, ζ-associated protein-70, and Src homology 2 domain-containing leukocyte protein-76 are required for TCR-induced microtubule-organizing center polarization. *J. Immunol.* 171:860–866.
24. Bunnell, S. C., V. Kapoor, R. P. Trible, W. Zhang, and L. E. Samelson. 2001. Dynamic actin polymerization drives T cell receptor-induced spreading: a role for the signal transduction adaptor LAT. *Immunity.* 14:315–329.
25. Misumi, Y., Y. Misumi, K. Miki, A. Takatsuki, G. Tamura, and Y. Ikehara. 1986. Novel blockade by brefeldin A of intracellular transport of secretory proteins in cultured rat hepatocytes. *J. Biol. Chem.* 261:11398–11403.
26. Negulescu, P. A., T. B. Krasieva, A. Khan, H. H. Kerschbaum, and M. D. Cahalan. 1996. Polarity of T cell shape, motility, and sensitivity to antigen. *Immunity.* 4:421–430.
27. Valitutti, S., S. Müller, M. Cella, E. Padovan, and A. Lanzavecchia. 1995. Serial triggering of many T-cell receptors by a few peptide-MHC complexes. *Nature.* 375:148–151.
28. Reichert, P., R. L. Reinhardt, E. Ingulli, and M. K. Jenkins. 2001. In vivo identification of TCR redistribution and polarized IL-2 production by naive CD4 T cells. *J. Immunol.* 166:4278–4281.
29. McGavern, D. B., U. Christen, and M. B. A. Oldstone. 2002. Molecular anatomy of antigen-specific $CD8^+$ T cell engagement and synapse formation in vivo. *Nat. mmunol.* 3:918–925.
30. Kupfer, A., G. Dennert, and S. J. Singer. 1985. The reorientation of the Golgi apparatus and the microtubule-organizing center in the cytotoxic effector cell is a prerequisite in the lysis of bound target cells. *J. Mol. Cell. Immunol.* 2:37–49.
31. Parsey, M. V., and G. K. Lewis. 1993. Actin polymerization and pseudopod reorganization accompany anti-CD3 induced growth arrest in Jurkat T cells. *J. Immunol.* 151:1881–1893.
32. Borroto, A., D. Gil, P. Delgado, M. Vicente-Manzanares, A. Alcover, F. Sanchez-Madrid, and B. Alarcon. 2000. Rho regulates T cell receptor ITAM-induced lymphocyte spreading in an integrin-independent manner. *Eur. J. Immunol.* 30:3403–3410.
33. Bunnell, S. C., D. I. Hong, J. R. Kardon, T. Yamazaki, C. J. McGlade, V. A. Barr, and L. E. Samelson. 2002. T cell receptor ligation induces the formation of dynamically regulated signaling assemblies. *J. Cell Biol.* 158:1263–1275.
34. Liu, H., M. Rhodes, D. L. Wiest, and D. A. A. Vignali. 2000. On the dynamics of TCR:CD3 complex cell surface expression and down-modulation. *Immunity.* 13:665–675.
35. Nicklas, R. B., S. C. Ward, and G. J. Gorbsky. 1995. Kinetochore chemistry is sensitive to tension and may link mitotic forces to a cell cycle checkpoint. *J. Cell Biol.* 130:929–939.